4

Autonomous Measurement System for Localization of Loss-Induced Perturbation Based on Transmission-Reflection Analysis

Vasily V. Spirin
División de Física Aplicada, CICESE,
Apdo. Postal 2732, CP 22860, Ensenada, B.C. México

1. Introduction

The highest state of the art in optical sensing is achieved with optical fiber distributed sensors that allow the measurement of a desired parameter along the test fiber (Hartog, 2000; Byoungho Lee, 2003). The regions where perturbations occur are usually localized by means of optical time-domain reflectometry (OTDR) or frequency domain reflectometry (OFDR) (Tsuji et al., 1995; Pierce et al., 2000; Venkatesh et al., 1990). All these methods utilize time- or frequency-modulated light sources that allow us to localize a number of perturbations along the test fiber simultaneously. Meanwhile, for some applications, it is important to detect and localize a rare but hazardous alarm condition which typically occurs as a single infrequent event, such as a pipe leak, fire or explosion.

For such applications, we proposed a novel simple and inexpensive measurement technique based on so-called transmission-reflection analysis (TRA) (Spirin et al., 2002a). Generally, the TRA method is based on the unique relationships between normalized transmitted and Rayleigh backscattered powers for different locations of the loss-induced disturbance along the sensing fiber. The TRA technique utilizes an unmodulated light source, power detectors and a sensing fiber. Localization of a strong disturbance with a maximum localization error of a few meters along a few km-long single-mode sensing fiber was demonstrated (Spirin et al., 2002b).

The paper presents a systematical review of our works in the TRA-sensing area. In the first parts of the paper we describe general ideas of the TRA, including principle of the operations of TRA-based sensors, localization errors examination, a transmission-reflection analysis for a distributed fiber-optic loss sensor with variable localization accuracy along the test fibre, and theoretical and experimental evidences that the TRA method can be modified for detection and localization of a number of perturbations that appear one after another at different positions along the test fiber.

In the final part we offer completely autonomous measurement system based on transmission-reflection analysis (AMS-TRA). This part includes design of the AMS-TRA system, thermal stability inspection, detailed analysis of experimental accuracy and localization errors, and implementation of the system for gasoline leak detection and localization.

2. Single Perturbation Localization

The basic idea of the TRA method is to localize the perturbation by using the unique relationships between normalized transmitted and Rayleigh backscattered powers of an unmodulated CW light source for different locations of the loss-induced disturbance along the sensing fiber. Indeed, if the bending losses occur at the remote-end of the sensing fiber (see Fig.1), an increase in the load leads to a proportional decrease of the transmitted power. However, it does not change the Rayleigh backscattered power, because all fiber length participate in backscattering and the launched power is the same such as for undisturbed fiber.

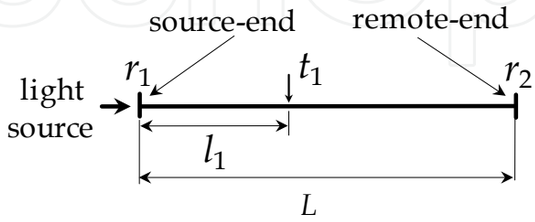

Fig. 1. Test fiber configuration for single perturbation; l_1 – perturbation location, t_1 – transmission of loss-inducing segment, r_1, r_2 – reflections from source- and remote-ends, L-test fiber length.

But if we bend the sensing fiber close to the source-end, the decrease in transmitted power is accompanied by a decrease in the Rayleigh backscattered power. Because in this case the launched into the fiber power is decreased and backscattered power is also decreased due to the induced losses.

Further, if we bend the sensing fiber in the middle, the first half of the fiber, which is closer to the source-end, scatters the light as well as half of undisturbed fiber, but the power scattered from the second half is less due to losses induced in the middle. So, for the identical loss-induced perturbations the value of the decrease in normalized backscattered power depends on the location of the excess loss region.

To find an analytical expression for calculation of the distance from the fiber source-end to the location of the loss region, we will analyze the configuration with two plain fiber sections whose lengths are l_1 and L-l_1 respectively, and a short fiber piece between them affected by a monitored condition (see Fig.1). Plain fiber sections possess Rayleigh scattering and attenuation due to light absorption and short fiber piece induces a losses. The power reflection coefficient of each Rayleigh scattering fiber segment can be calculated as (Gysel & Staubli, 1990; Liaw et al., 2000):

$$R(\delta l_i) = S(\alpha_s / 2\alpha)[1 - \exp(-2\alpha\delta l_i)], \tag{1}$$

where α_s is the attenuation coefficient due to Rayleigh scattering, α is the total attenuation coefficient of the test fiber, δl_i is the length of the i-th fiber segment, and recapture factor S for the fiber is defined as (Brinkmeyer, 1980):

$$S = b(n_1^2 - n_2^2)/n_1^2 , \tag{2}$$

where b depends on the waveguide property of the fiber and is usually in the range of 0.21 to 0.24 for single-mode step-index fiber (Brinkmeyer, 1980), n_1 and n_2 are the refractive indices of the fiber core and cladding, respectively.
Introducing a parameter $S_\alpha = S(\alpha_s/2\alpha)$, the transmission and backscattering coefficients of plain fiber sections can be written as $T_i = exp\ (-\alpha\delta l_i)$ and $R_i = S_\alpha(1\text{-}exp(-2\alpha\delta l_i)$, respectively. The short fiber piece is affected by monitored conditions which introduce additional light losses. A transmission of short fiber piece is $t_1 \le 1$. Let us assume that the scattering is relatively weak and the portion of the scattered light is very small. This allows us to simplify the analysis, neglecting multiple scattering in both directions. The reflections with coefficients r_1 and r_2 from the fiber source- and remote-ends, respectively, have to be taken into account because even a weak reflection can be comparable to the back scattering. However, we can assume that $r_{1,2} << 1$ and neglect multiple reflections as well.
In this case, the transmission T and back-scattering R coefficients of this optical system can be written as:

$$T = T_1 t_1 T_2 = t_1 \mathrm{e}^{-\alpha L}\ , \tag{3}$$

$$R = r_1 + S_\alpha(1 - e^{-2\alpha l_1}) + T_1^2 t_1^{\,2} S_\alpha(1 - e^{-2\alpha(L-l_1)}) + T_1^2 t_1^2 T_2^2 r_2. \tag{4}$$

Normalized transmitted T_{norm} and backscattered R_{norm} coefficients are defined as:

$$T_{norm} = \frac{T}{T_{\max}} = t_1, \tag{5}$$

$$R_{norm} = \frac{R}{R_{\max}} = \frac{S_\alpha + r_1 - (S_\alpha - r_2)t_1^2 e^{-2\alpha L} - S_\alpha(1 - t_1^{\,2})e^{-2\alpha l_1}}{S_\alpha + r_1 - (S_\alpha - r_2)e^{-2\alpha L}}, \tag{6}$$

where $T_{\max}$ is the maximum transmittance of initially undisturbed sensing fiber when t_1 =1,

$$T_{\max} = \mathrm{e}^{-\alpha L}\ , \tag{7}$$

and $R_{\max}$ is the maximum back-scattering coefficients of undisturbed optical system

$$R_{\max} = S_\alpha + r_1 - (S_\alpha - r_2)e^{-2\alpha L}. \tag{8}$$

The relationship between the normalized transmitted T_{norm} and Rayleigh backscattered R_{norm} powers for single perturbation can be expressed from (5-6) as:

$$T^2{}_{norm} = \frac{(S_\alpha + r_1)(R_{norm} - 1) - R_{norm}(S_\alpha - r_2)e^{-2\alpha L} + S_\alpha e^{-2\alpha l_1}}{S_\alpha(e^{-2\alpha l_1} - e^{-2\alpha L}) + r_2 e^{-2\alpha L}}. \tag{9}$$

To localize the perturbation with the proposed method, we need to find a parametric curve that passes through the point with coordinates equal to the measured normalized Rayleigh

backscattered and transmitted powers. The location of the loss region can also be found directly from Eqn. (9) as:

$$l_1 = -\frac{1}{2\alpha}\ln\frac{(1-R_{norm})(S_\alpha + r_1) + (R_{norm} - T_{norm}^2)(S_\alpha - r_2)e^{-2\alpha L}}{S_\alpha(1-T_{norm}^2)}. \tag{10}$$

Therefore, the measurement of the normalized transmitted and backscattered powers, as well as the knowledge of the fiber attenuation coefficients α and α_s, provide the calculation of the distance l_1 from the fiber source-end to the fiber section with induced losses.
The slope of dependence of normalized backscattered power R_{norm} versus the square of normalized transmitted power T^2_{norm} can be found from Eqn. (9) as:

$$\frac{\partial R_{norm}}{\partial(T^2_{norm})} = \frac{S_\alpha(e^{-2\alpha l_1} - e^{-2\alpha L}) + r_2 e^{-2\alpha L}}{S_\alpha + r_1 - (S_\alpha - r_2)e^{-2\alpha L}}. \tag{11}$$

As we can see this slope uniquely depends on perturbation location l_1. Therefore, the location of the single perturbation can be found from experimentally measured slope as:

$$l_1 = \frac{1}{2\alpha}\ln\left[\frac{S_\alpha}{(S_\alpha + r_1)\frac{\partial R_{norm}}{\partial(T^2_{norm})} + (r_2 - S_\alpha)e^{-2\alpha L}\left(\frac{\partial R_{norm}}{\partial(T^2_{norm})} - 1\right)}\right]. \tag{12}$$

The relationship between normalized Rayleigh backscattered power R_{norm} and the square of normalized transmitted power T^2_{norm} is almost linear for a single perturbation which affects the test fiber in any location (see Eqn. (9)). Fig.2 shows the result of the numerical calculation of these relationships when additional losses occur at distances $l_{1,n} = n\Delta l$ from the source-end of the test fiber, where n = 0,1…10, and the interval between bending locations Δl = 284.4 meter. Transmitted and backscattered powers were normalized with respect to their initial undisturbed values. A typical value for b equal to 1/4.55 for single-mode fibers (Beller, 1998) was used in the calculations. Reflections from the source-end and the remote-end of the sensing fiber, which are respectively equal to $4.7\text{x}10^{-6}$ and $1.5\ \text{x}10^{-5}$ in our experiment, were also taken into account in the calculations.
For the verification of the proposed method we use firstly a laboratory experimental setup. The schematic diagram of the TRA based fiber-optic sensor is shown in Fig. 3. A continuous wave (CW) light emitted by a amplified spontaneous emission (ASE) optical fiber source operating near 1550 nm wavelength with a linewidth of few nm was launched into a 2.844 km-long standard single mode SMF-28 fiber through 3 dB coupler. The launched optical power was about 1.1 mW, and the attenuation coefficient of the test fiber, which was measured with OTDR, was equal to 0.19 dB/km. An optical isolator was used to cancel back reflections influence on ASE source. An immersion of all fiber ends was employed in order to reduce back reflections. Standard power detectors were used to measure the transmitted

and Rayleigh backscattered powers. We also take into account the ASE power instability by measuring a source power directly (see Fig.3).

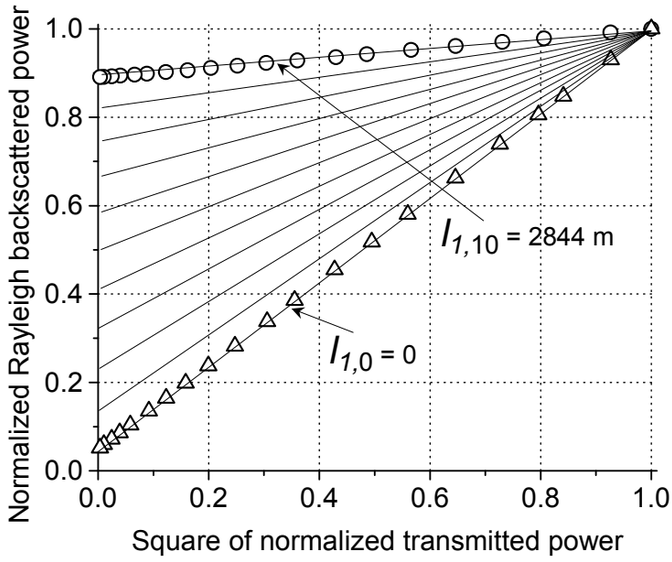

Fig. 2. Relations between normalized Rayleigh backscattered power and the square of normalized transmitted power when additional losses occur at distances $l_{1,n} = n\Delta l$ from the source-end of the test fiber, where n = 0,1…10, and the interval between bending locations Δl = 284.4 m. (o, Δ - experimental results, and solid lines – theoretical dependencies).

To induce the bending losses in the sensing fiber, we used bending transducer, which is also shown schematically in Fig.3. By tuning the bending transducer we changed the normalized transmitted power from its initial undisturbed value equal to 1 up to more than -30 dB. The bending losses were induced near source-end and near remote-end of the test fiber.

A good agreement between experimental data and theory was obtained for (α_s/α) = 0.68, that corresponds attenuation coefficient due to Rayleigh scattering α_s equal to 0.13 dB/km that is quite reasonable for the fiber with total attenuation coefficient α = 0.19 dB/km (Beller, 1998).

Experimentally measured slopes for the bending losses, which were induced near remote - and source -ends of the test fiber are equal to 0.109, and 0.95, correspondingly. These values well agree with the values calculated using Eqns. (11), which are equal to 0.108, and 0.96, respectively.

So, for standard telecommunication single mode fibers the TRA method demonstrates concord between calculated and experimentally measured data practically without any fitting parameters. Even using for simulation a typical values of unknown recapture factor S and relation (α_s/α) between Rayleigh-induced and total losses in the fiber guarantee quit reasonable conformity.

Concluding this section we can declare that TRA method provides new opportunity for the localization of loss-induced alarm-like perturbation along few km-length fibers by uncomplicated measuring of transmitted and Rayleigh backscattered powers of an unmodulated CW light.

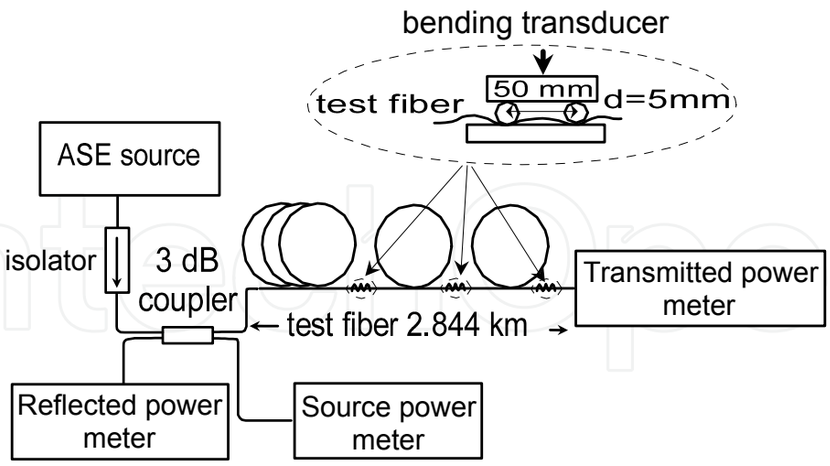

Fig. 3. Schematic diagram of laboratory setup of TRA fiber-optic sensor.

3. Multi-Point Perturbations Localization

Let us now verify that any number of consecutive perturbations can be localized with the TRA method. The proof will be done by mathematical induction. In our analysis we consider the test fiber with the same properties and parameters as in previous case. But now we use a configuration with a number of plain Rayleigh-scattering fiber sections separated by a number of short loss-inducing fiber pieces with transmissions $t_i \le 1$ (see Fig.4), (Spirin, 2003).

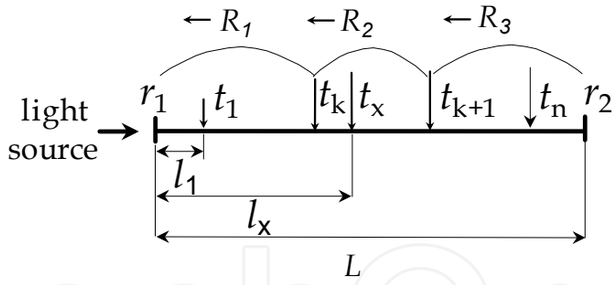

Fig. 4. Test fiber configuration for multi-point perturbations; $t_1 \div t_n$ – transmission of initially disturbed loss-inducing segments, t_x transmission of currently disturbed segment, r_1, r_2 – reflections from source- and remote-ends.

Let us assume that according to the principle of mathematical induction we already determined the values and locations of the first n perturbations and demonstrate that we can find a position of next (n+1)-th perturbation without ambiguity. Here we consider only the perturbations that appear one after another at different positions along the test fiber. So, at the current moment all initial n perturbations induce fixed known losses at known locations and only a new (n+1)-th perturbation can modify the reflectivity and transmittance of the test fiber.

Because we know the positions and values of all n initial perturbations, we can number these according their positions along the test fiber (see Fig.4). We also can suppose without loss of generality that a new perturbation is located at distance l_x between k-th and (k+1)-th initial perturbations, where k is unknown.
The transmittance of initial n loss-inducing short segments which are located at distances l_j from the source-end is $t_j \le 1$, where j = 1, n. The transmittance of unknown loss-inducing segment which is located at distance l_x is t_x. Assuming that the scattering and reflections from the fiber ends are relatively weak and neglecting multiple scattering and reflections in both directions, the normalized power reflection coefficient of the optical system can be calculated as:

$$R_{norm} = \frac{R_1 + R_2 + R_3}{R_{\max}}. \tag{13}$$

In Eqn. (13) R_1 corresponds to Rayleigh backscattering from segments placed on the left of unknown perturbation plus Fresnel reflection from the source-end of the test fiber

$$R_1 = r_1 + S_\alpha \sum_{i=0}^{k-1} \{T_{l_i}^2 (1 - e^{-2\alpha(l_{i+1} - l_i)}) \prod_{j=0}^{i} t_j^2\}, \tag{14}$$

R_2 is Rayleigh backscattering coefficient of two segments, which are placed around the unknown perturbation

$$R_2 = S_\alpha \prod_{j=0}^{k} t_j^2 \{T_{l_k}^2 [1 - e^{-2\alpha(l_x - l_k)}] + T_{l_x}^2 [1 - e^{-2\alpha(l_{k+1} - l_x)}] t_x^2\}, \tag{15}$$

and R_3 is power reflection coefficient for segments which are placed on the right of disturbed region plus term related to reflection from the remote-end of the test fiber

$$R_3 = t_x^2 \{S_\alpha \sum_{i=k+1}^{n} T_{l_i}^2 [1 - e^{-2\alpha(l_{i+1} - l_i)}] \prod_{j=0}^{i} t_j + T_L^2 r_2 \prod_{j=0}^{n} t_j^2\}, \tag{16}$$

where $T_{li} = \exp(-\alpha l_i)$ is the transmission coefficient of fiber segment with length l_i (see Fig.4), r_1, r_2 are the reflections coefficients from the fiber source- and remote-ends, respectively.

In the expressions (14 -16) we assign that: $l_0 \equiv 0$, $t_0 \equiv 1$ and, $l_{n+1} \equiv L$. We should emphasize that the condition $t_0 \equiv 1$ does not means that perturbation cannot appear near the source-end of the test fiber. The disturbance can affect the fiber near the source-end but it should be marked as first perturbation with transmittance t_1 at $l_1 = 0$ distance.
The normalized transmitted coefficient of the optical system which is affected by all n+1 perturbations is defined as:

$$T_{norm}^2 = t_x^2 \prod_{j=1}^{n} t_j^2. \tag{17}$$

Note that the changes of first n perturbations are almost finished before a new one is started, so t_j = constant for j =1, n. Therefore, the total normalized transmitted power for all n+1 perturbations T^2_{norm} can change only due to the change of current perturbation, and differential $\partial(T^2_{norm})$ is:

$$\partial(T^2_{norm}) = \partial(t_x^2)\prod_{j=1}^{n} t_j^2. \tag{18}$$

The derivative of normalized backscattering power with respect to the square of normalized transmitted power is expressed as:

$$\frac{\partial R_{norm}}{\partial(T^2_{norm})} = \frac{}{R_{\max}}[\frac{\partial R_1}{\partial(T^2_{norm})} + \frac{\partial R_2}{\partial(T^2_{norm})} + \frac{\partial R_3}{\partial(T^2_{norm})}] =$$

$$= \frac{}{R_{\max}\prod_{j=0}^{n} t_j^2}\{S_\alpha \prod_{j=0}^{k} t_j^2[e^{-2\alpha l_x} - e^{-2\alpha l_{k+1}}] + S_\alpha \sum_{i=k+1}^{n}[e^{-2\alpha l_i} - e^{-2\alpha l_{i+1}}]\prod_{j=0}^{i} t_j + T_L^2 r_2 \prod_{j=0}^{n} t_j^2\}. \tag{19}$$

This derivative (or slope of dependence of normalized backscattering power versus the square of normalized transmitted power) depends only on the backscattering from the plain segments which are located on the right side of unknown perturbation. The plain segments, which are located on the left of the unknown perturbation, do not affect the slope.
Let us introduce for $0 \le k \le n$+1 an auxiliary function F(k, n):

$$F(k,n) = \frac{}{R_{\max}\prod_{j=0}^{n} t_j^2}\{S_\alpha \sum_{i=k}^{n}[e^{-2\alpha l_i)} - e^{-2\alpha l_{i+1}}]\prod_{j=0}^{i} t_j + T_L^2 r_2 \prod_{j=0}^{n} t_j^2\}. \tag{20}$$

The auxiliary function has a similar structure as the expression for the slope (see Eqn. 19) and it is decreasing with k for any n (see Fig. 5).
The contribution in the slope due to backscattering from segment [l_x, l_{k+1}] which is associated with the term [exp(-2αl_x) - exp(-2αl_{k+1})] in Eqn. (19) is less than the possible contribution due to backscattering from full segment [l_k, l_{k+1}] which is associated with term [exp(-2αl_k) - exp(-2αl_{k+1})] in Eqn. (20). Comparing Eqns. (19) and (20) we can conclude that, if the measured value of the slope for unknown perturbation satisfies the relation:

$$F(k^*+1,n) < \frac{\partial R_{norm}}{\partial(T^2_{norm})} < F(k^*,n), \tag{21}$$

the unknown perturbation is located between k^*-th and (k^*+1)-th initial perturbations (see Fig. 5).
Note that, if the measured slope of the unknown perturbation is equal to $F(0,n)$, the new perturbation affects the testing fiber near the source-end of the test fiber. If the slope is equal to $F(n+1,n)$ = exp(-2αL)r_2/R_{max}, the unknown disturbance is located near the remote-end of the test fiber.

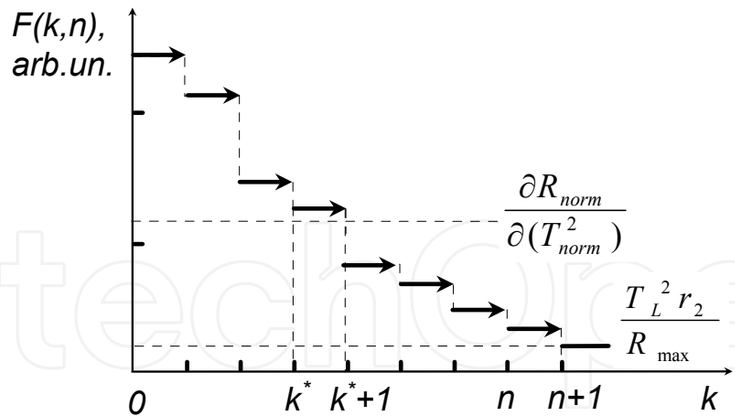

Fig. 5. Preliminary localization of (n+1)-th perturbation with auxiliary function $F(k,n)$.

Finally, the exact location of sought-for short loss segment can be found as:

$$l_x = \frac{1}{2\alpha}\ln\left\{\frac{S_\alpha}{\left[\frac{\partial R_{norm}}{\partial(T^2_{norm})} - F(k^*+1,n)\right]R_{\max}\prod_{j=k+1}^{n} t_j^2 + S_\alpha e^{-2\alpha l_{k^*+1}}}\right\}. \quad (22)$$

In the previous section we have presented the method for single perturbation localization with the TRA technique. Now we have demonstrated the algorithm for localization of a new perturbation when the values and locations of all initial n perturbations are known. Therefore, according to the principle of mathematical induction we have demonstrated that the TRA method can be implemented for the localization of any number of consecutive perturbations.

Fig. 6 shows experimental dependencies of normalized Rayleigh backscattered powers versus the square of normalized transmitted powers for the bending losses consequently induced near the remote- and source-ends of test fiber. Measurements were performed as follows. Initially, the perturbation occurred near the remote-end of test fiber. The increase of the losses leads to decrease of transmitted power (line A in Fig.6). When the square of normalized transmittance decreases to the value equal to 0.241 of its initial undisturbed magnitude, we stop to increase the bending losses. Afterwards, keeping constant losses near the remote-end, we induce additional losses near the source-end of test fiber. This loading continues until the value of the square of normalized transmittance decreases to the 0.061 (line B). Then, keeping the same value of losses near the source-end, we gradually remove the losses near the remote-end of test fiber (line C in Fig. 6). Finally, by eliminating the losses near the source-end, all parameters return to their initial undisturbed values (line D).

All experimental dependencies presented in Fig.6 possess linear behavior. Experimental data show good agreement with theoretical prediction. Namely, experimental dependencies A and D practically coincide with the calculated dependencies using Eqn. 9 (see Fig. 2 and Fig. 6). Experimentally measured slopes for lines A, B, C and D which are equal to 0.109, 3.63, 0.109 and 0.955, correspondingly, agree with the values calculated using Eqns. (11) and (19) which are equal to 0.108, 3.631, 0.108 and 0.957, correspondingly.

Note that the slopes were the same for loading and unloading dependencies. The localization errors that were estimated from the difference between measured and calculated slopes do not exceed 2 meters for any location of perturbation. We should note, however, that in practice, different noise origins and system imperfections such as temporal drifts of fiber and photodetectors parameters, additional uncontrolled losses, etc. may also contribute to the decrease of accuracy. More complete analysis of localization accuracy with the TRA method will be conducted latter.

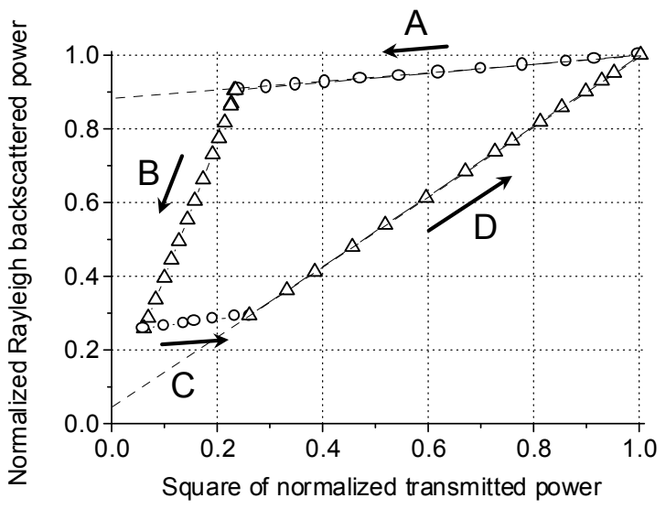

Fig. 6. Relations between normalized Rayleigh backscattered power and the square of normalized transmitted power for the bending losses consequently induced near the remote- and source-ends of test fiber.

Therefore, the TRA method can be implemented for the localization of any number of consecutive perturbations which occur one after another along the test fiber during the monitoring period. In contrast to the OTDR the proposed method cannot be used for the localization of the perturbations in an already installed fiber-optical system that already has many induced losses. The other natural question to be addressed about the TRA method is: what happens if two perturbations affect the test fiber simultaneously? To answer this question, consider calculated dependence of normalized Rayleigh backscattered power versus the square of normalized transmitted power for two equal perturbations which induce the losses near the source- and remote-ends at same time (curve A+D in Fig.7).
The dependence exhibits clear nonlinear behavior. As was shown above for any number of consecutive perturbations this dependence should be linear. Fig. 7 also shows normalized Rayleigh backscattered power versus the square of normalized transmitted power for the perturbations that affect the testing fiber one after another near the remote (line A) and source (line D) ends. Both last dependencies exhibit clear linear behavior. The nonlinear behavior of dependencies of normalized Rayleigh backscattered power versus the square of normalized transmitted power indicates that testing fiber is affected by two or more perturbations simultaneously.

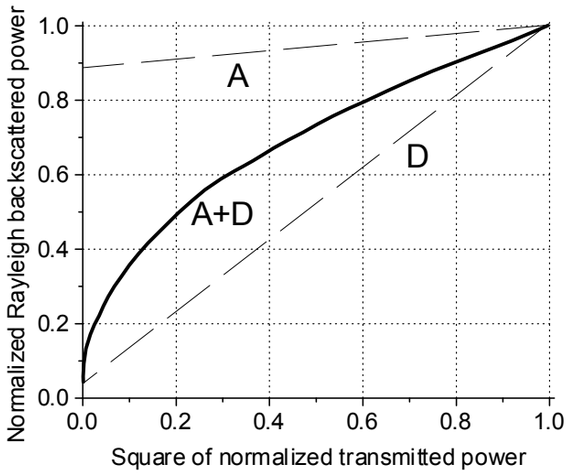

Fig. 7. Relations between normalized Rayleigh backscattered power and the square of normalized transmitted power for two perturbations synchronously (A+D) and independently (A and D) induced near the remote- and source-ends of test fiber.

Using the particular dependence that is shown in Fig. 7 (curve A+D), it is possible to localize at least one perturbation. Indeed, the value of normalized Rayleigh backscattered power at the point when normalized transmitted power is equal to 0 directly shows the location of nearest to the source-end perturbation. Therefore, analyzing the curve A+D, we can conclude that two perturbations affect the test fiber simultaneously and one of the perturbations induces the losses near the source-end. Nevertheless, the complete analysis of different scenarios, even for two synchronous events, is noticeably complicated and is beyond the scope of this paper.

4. Localization Accuracy with TRA Method

The accuracy of excess loss localization with TRA method strongly depends on the value of the induced loss. With TRA method it is easy to localize strong perturbation, but the localization of weak perturbation requires higher accuracy of the transmitted and Rayleigh backscattered powers measurements.
Indeed, normally we measure normalized power transmission and reflection coefficients with some errors. So, the measurements are positioned mainly inside an area: $T_{norm} \pm \sigma_{Tnorm}$ and $R_{norm} \pm \sigma_{Rnorm}$, where σ_{Rnorm} and σ_{Tnorm} are deviations of normalized reflected and transmitted powers, respectively. Let us characterize this measurement area in the space T^2_{norm} - R_{norm} by a measurement-rectangular with sides equal to $2\sigma_{T^2norm}$ and $2\ \sigma_{Rnorm}$, where σ_{T^2norm} is deviation of square of normalized transmitted power (see Fig.8). The size of the rectangular indicates the accuracy of the measurements. Smaller measurement-rectangular corresponds to higher measurement accuracy. Fig.8 also repeat dependences already presented in Fig. 2 for the losses induced at different locations with interval Δl = 284.4 m.
Every line which is intersecting the measurement-rectangular corresponds to one of the possible local position of the perturbation. Therefore the localization error depends on the

number of the intersecting lines. As we can see for very week losses nearly all lines cross the measurement-rectangular that means that we need significantly higher accuracy of the measurements for the correct localization. For the strong losses the localization error reaches its minimum with the TRA method. In contrast to this, the accuracy of localization of loss with the standard OTDR technique mainly depends on the duration of the optical test pulse and is practically independent on the value of loss.

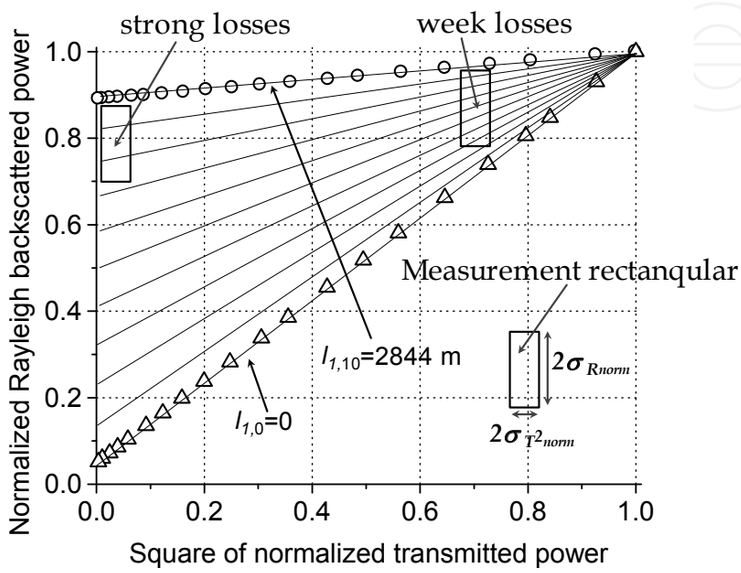

Fig. 8. Localization accuracy with TRA method.

Fig. 9. shows the relative localization error calculated geometrically using the data, which are presented in Fig.8.

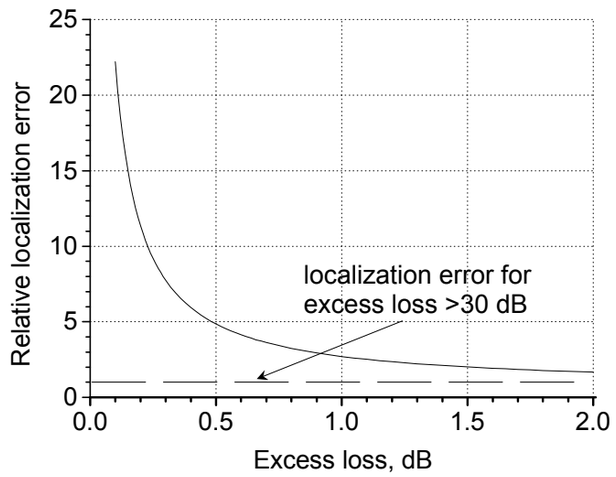

Fig. 9. Relative localization error versus excess loss for the TRA method.

Relative localization error was determined as localization error divided by their value for the loss that decreased the fiber transmission by more than 30 dB. As we can see the localization error for weak loss significantly exceeds the localization error for strong one. If the localization errors for very strong perturbation are equal to ±1meter the localization errors for 1 and 0.1 dB induced loss are equal to ±3 meters and ±22 meters, respectively.
The measurement range and maximum allowable loss for the TRA and OTDR methods are likely to be the same, because both methods measure the Rayleigh backscattering power and the maximum range for both methods is namely restricted by the attenuation of test fiber.
Now, let us examine some special features of the localization accuracy with the TRA method analytically. Firstly let us demonstrate that if the influence of coherent effects is negligibly small, the TRA method can be used for any arbitrary distribution of the reflectivity along the test fiber.
Indeed, let us consider a fiber with total length L, initial transmission $T_{\max}= T(L)$ and an arbitrary distribution of power reflectivity $R(z)$ along the fiber. The reflectivity $R(z)$ is monotonically non-decreasing function in interval [0, L] if we neglect any coherent effects. The reflectivity $R(z)$ can be measured as the dependence of the reflected power versus the distance z where very strong loss ($t_{norm} \cong 0$) is induced. A derivative $\partial R(z)/\partial z$ can be interpreted as a differential reflectivity that also has an arbitrary distribution along the test fiber. Reflectivity inside the fiber can be induced by Raleigh backscattering or any other way including imprinting of Bragg gratings inside the fiber.
Taking into account the reflection from the ends of the sensing fiber, total power reflection coefficient of the initially undisturbed optical system can be expressed as:

$$R_{\max} = r_1 + R(L) + T^2(L) r_2, \tag{23}$$

where $R(L)$ *is* power reflection coefficient of all fiber.

Let a short fiber piece located at a distance $l_1 \le L$ induce a loss under influence of a monitored condition. Neglecting coherent effects, multiple scattering and re-reflection in both directions due to its relative weakness, and supposing that no additional reflection comes from loss region the normalized power reflection coefficient R_{norm} of the optical system with a single disturbance located at distance l_1 can be written as:

$$R_{norm} = \frac{r_1 + R(l_1) + [R(L) - R(l_1)] T^2(l_1) T_{norm}^2 + T^2(L) T_{norm}^2 r_2}{r_1 + R(L) + T^2(L) r_2}, \tag{24}$$

where T_{norm} is the normalized power transmission coefficient of the optical system with excess loss, $T(l_1)$ and $R(l_1)$ are transmission and power reflection coefficient of the fiber segment with length l_1, respectively.

Measurands T_{norm} and R_{norm} are normalized by their initial undisturbed values $T_{\max}$ and $R_{\max}$, respectively. As follow from Eqn. (24) the dependence between R_{norm} and T^2_{norm} is linear with unique slopes for different locations of the perturbation l_1 along the test fiber.

Therefore, with the TRA method the single loss perturbation can be localized by measuring the slope $\partial R_{\text{norm}} / \partial(T^2_{\text{norm}})$ for any arbitrary distribution of the reflectivity $R(z)$ along the test fiber.
Neglecting Fresnel reflections from both fiber ends ($r_1 = r_2 = 0$) and losses in undisturbed fiber ($T(l_1)=1$) we can express normalized power reflection coefficient of the segment with length 1_1 from Eqn. (24) as:

$$R_N(l_1) = \frac{R(l_1)}{R(L)} = \frac{R_{norm} - T^2_{norm}}{1 - T^2_{norm}}. \tag{25}$$

As a result, the location of the perturbation can be written as:

$$l_1 = R_N^{-1}\left(\frac{R_{norm} - T^2_{norm}}{1 - T^2_{norm}} \right), \tag{26}$$

where R_N^{-1} is inverse function.

In order to find the loss locacion l_1 from Eqn. (26) we needs to know the function R_N^{-1}, but even without this knovelege we can estimate some features of the localization accuracy. Indeed, for independently measured normalized reflected and transmitted powers, the standard deviation of the disturbance location σ_{l1} can be estimated as:

$$\sigma^2_{l_1} = \left(\frac{\partial R_N^{-1}}{\partial R_{norm}} \right)^2 \sigma^2_{R_{norm}} + \left(\frac{\partial R_N^{-1}}{\partial T_{norm}} \right)^2 \sigma^2_{T_{norm}}, \tag{27}$$

where $\sigma_{R_{norm}}$ and $\sigma_{T_{norm}}$ are standard deviations of normalized reflected and transmitted powers, respectively.

Here we also assume that errors for T_{max} and R_{max} were significantly less than ones for T_{norm} and R_{norm}, because an averaging time for an initial measurements can significantly exceeds the averaging time at normal-mode regime.
Substituting expression (26) in Eqn. (27) we can obtain:

$$\sigma_{l1} = \frac{1}{(1 - T^2_{norm}) \left. \frac{\partial R_N(z)}{\partial z} \right|_{z=l_1}} \sqrt{\sigma^2_{R_{norm}} + \left(\frac{2T_{norm}[R_{norm} - 1]}{1 - T^2_{norm}} \right)^2 \sigma^2_{T_{norm}}}. \tag{28}$$

As it follow from Eqn. (28) the accuracy of localization with the TRA method depends on normalized differential reflectivity $\partial R_N(z)/\partial z$ at the point of measurement l_1. Larger differential reflectivity corresponds to highter accuracy of loss localization.

Therefore, with the TRA method we can achieve variable accuracy distribution along the test fiber with the proper profile of the normalized differential reflectivity.
Enhanced localization accuracy inside several critical intervals can be provided, for example, by imprinting of very week Bragg gratings inside these intervals (Spirin et al., 2004).
Note that the total resolution of the TRA sensor also depends on the uniformity of the waveguide, scattering and loss properties of the test fiber. However, the precise value of the reflectivity $R(z)$ can be directly measured by inducing strong losses at exactly-known locations along the test fiber or, probably, by precise OTDR measurements.
Rayleigh backscattering phenomena meets the condition discussed above because the Rayleigh backscattered power coefficient $R(l_1)$ is independent of the coherent properties of the incident light (Gysel & Staubli, 1990; Liaw et al., 2000):

$$R(l_1) = S_\alpha[1-\exp(-2\alpha l_1)]. \tag{29}$$

Let us estimate the localization errors for the Rayleigh backscattered fiber numerically. Neglecting Fresnel reflections from both fiber ends ($r_1 = r_2 = 0$) we can express the location of the perturbation from Eqn. (10) as:

$$l_1\left(R_{norm}, T_{norm}\right) = \frac{1}{2\alpha}\ln\left\{\frac{1-T_{norm}^2}{1-R_{norm}+R_{norm}e^{-2\alpha L}-T_{norm}^2 e^{-2\alpha L}}\right\}. \tag{30}$$

The perturbation location depends on two measurands T_{norm} and R_{norm} which can be defined experimentally with some errors. For independently measured reflected and transmitted powers the error in location can be found directly from Eqn. (30) as:

$$\sigma^2{}_{l_1} = \left(\frac{\partial l_1}{\partial R_{norm}}\right)^2 \sigma^2_{R_{norm}} + \left(\frac{\partial l_1}{\partial T_{norm}}\right)^2 \sigma^2_{T_{norm}}. \tag{31}$$

Fig.10. shows the calculated with Eqn. (31) localization error versus transmission for two different local positions of the perturbation along 10 km-length test fiber. In the simulation we used standard deviations of the reflected σ_{Rnorm} and transmitted σ_{Tnorm} powers equal to 0.005 and 0.0005, respectively. As we can see the location error depends on the distance where the perturbation takes place and strongly depends on the value of the induced loss. Once again, the localization of a weak perturbation with TRA method requires more accurate measurements of the transmitted and Rayleigh backscattered powers. More precise measurements can be provided by increasing the averaging time, especially for the reflected power because typically the Rayleigh backscattered power is significantly smaller and noisiness than the transmitted one.
Consequently, the TRA method is well adjusted on detection and localization of single strong enough perturbation. However we have also demonstrated that the TRA method provides wide range of localization accuracy for weak and strong loss-inducing perturbations. It was shown that the required accuracy distribution along the test fiber can be achieved with the appropriate profile of the normalized differential reflectivity $\partial R_N(z)/\partial z$.

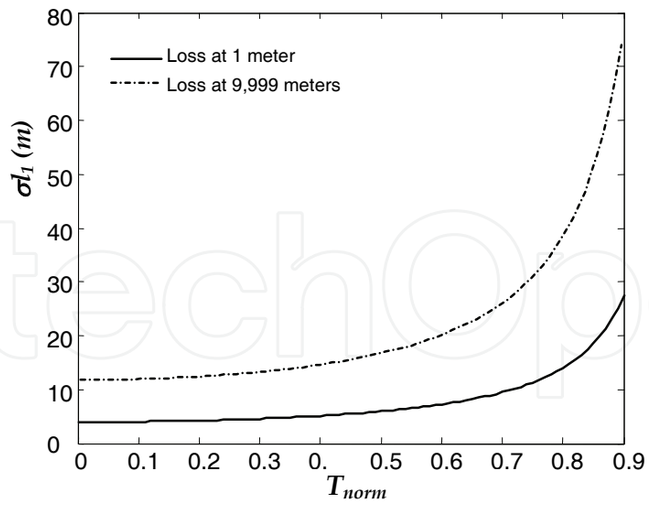

Fig. 10. Localization error versus transmission for 10 km-length test fiber.

5. Autonomous Measurement System

The section describes first completely autonomous measurement system based on transmission-reflection analysis (AMS-TRA). The autonomous system utilizes simple optical scheme with low-cost 2 mW Fabry-Perot (FP) diode laser and original data acquisition and processing system (Spirin et al., 2007). The schematic diagram of AMS-TRA prototype is shown in Fig. 11. CW light emitted by a FP laser operating in few longitudinal modes at 1550 nm with a total linewidth of few nm was launched into a standard single mode SMF-28 test fiber through 3 dB coupler.

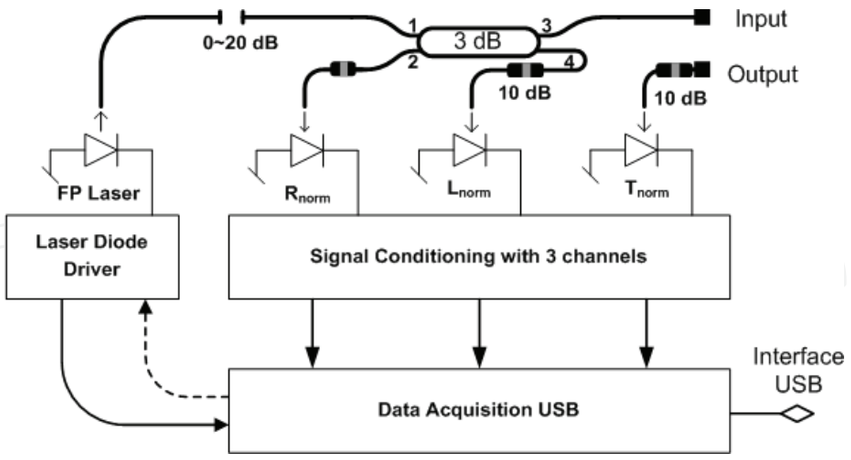

Fig. 11. Schematic diagram of fiber-optic sensor

The launched optical power was about 1 mW, and the measured with OTDR attenuation coefficient of the test fiber was equal to 0.19 dB/km. The angled physical contact (APC) connectors were used to cancel back reflections influence on the FP laser.

Three power detectors with specially designed preamplifiers and filters were used to measure the transmitted (T), Rayleigh backscattered (R), and laser (L) powers.
Fig.12 shows the overview of AMS-TRA system with short peace of sensing cable for hydrocarbon leak detection. After digitization data transferred to PC via USB interface. The data acquisition, signal processing, and the indication of the event location on the map is done by specially designed software.

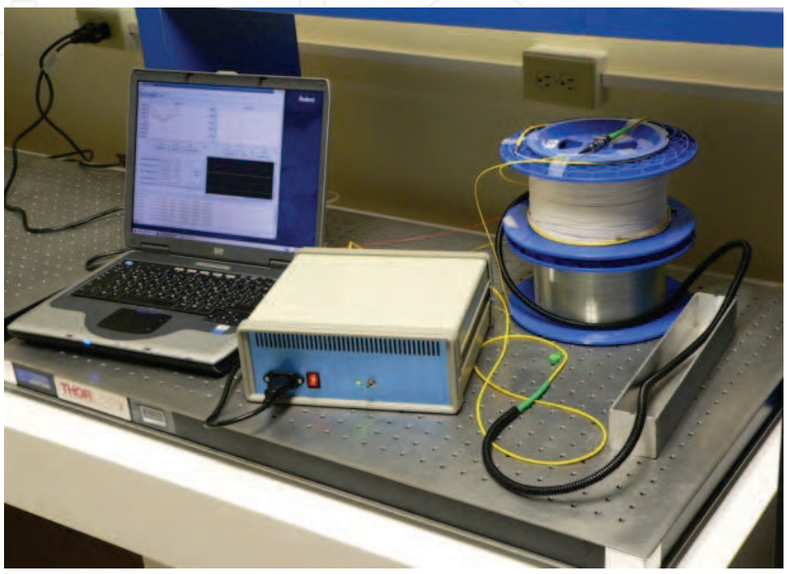

Fig. 12. AMS-TRA prototype.

5.1 Thermal Stability

As we found, considerable problem with our first AMS-TRA prototype version is associated with ambient temperature influence. Fig.13 shows the variation of the measurands T_{norm}, R_{norm} and L_{norm} during 14 hours.

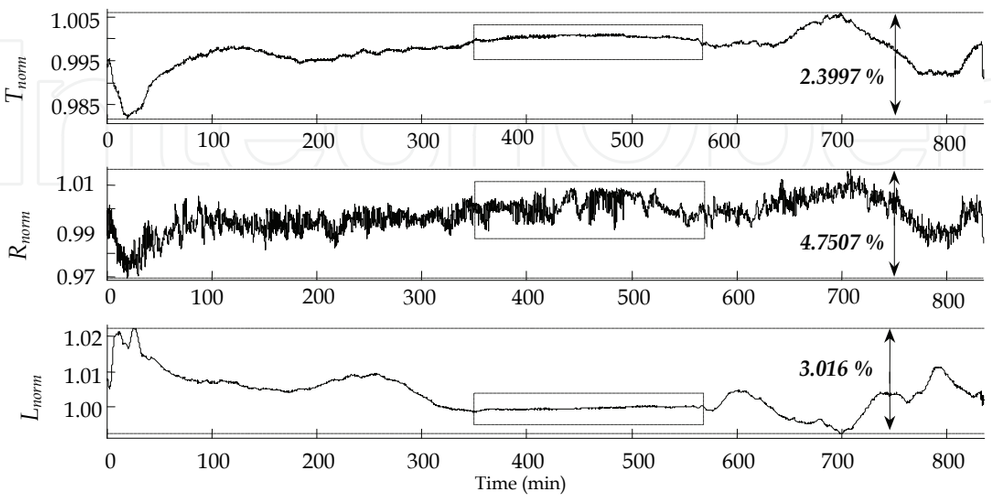

Fig. 13. Measurands variations during 14 hours

Here L_{norm} is directly measured FP laser power (see Fig.11) normalized on its initial value. Smallest variations of the measured values were recorded during the night when the temperature in the room was stable (see Fig. 13).
Significant measurands variations were also recorded every time after AMS-TRA is turn on. Fig.14 shows measurands variations from the moment when an electrical power was switch on. The losses were induced near remote-end of 1.3 km-length test fiber. The measurands became stable only after 1 hour (see Fig.14) when the temperature inside the prototype box stabilized.

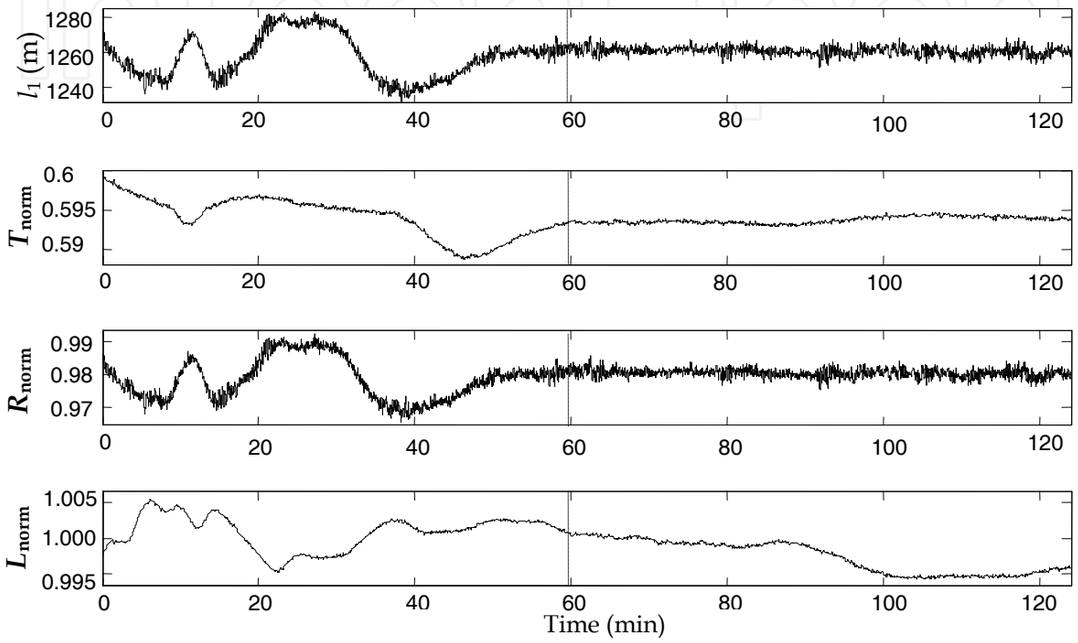

Fig. 14. Measurands variations after power is switch on.

In order to get most temperature-sensitive points we heat different optical and electrical parts of the prototype on 10° C. As we found the most temperature-critical elements are standard optical connectors. However it is possible to eliminate the problem by using special temperature insensitive connectors or simply splicing all fibers.

5.2 Localization Error Measurements

To estimate the accuracy of the perturbation localization with the AMS-TRA prototype, we induced gradually increasing and decreasing perturbations near source- and remote-end of the 1.3 km-length SMF-28 test fiber. Fig.15 shows variation of perturbation location l_1 and other measurands with change the losses near the source-end of the test fiber. For the strong losses that surpass 3dB the variation of l_1 about ±2 meters was recorded.
Fig.16 shows calculated and measured localization errors for 1.3 km-length test fiber versus normalized transmitted power. In the simulation we used experimentally measured standard deviations of the reflected and transmitted powers equal to 0.0015 and 0.0003, respectively. As we can see measured errors for the strong perturbations do not exceed ±5 m for the losses induced near remote-end of the test fiber.

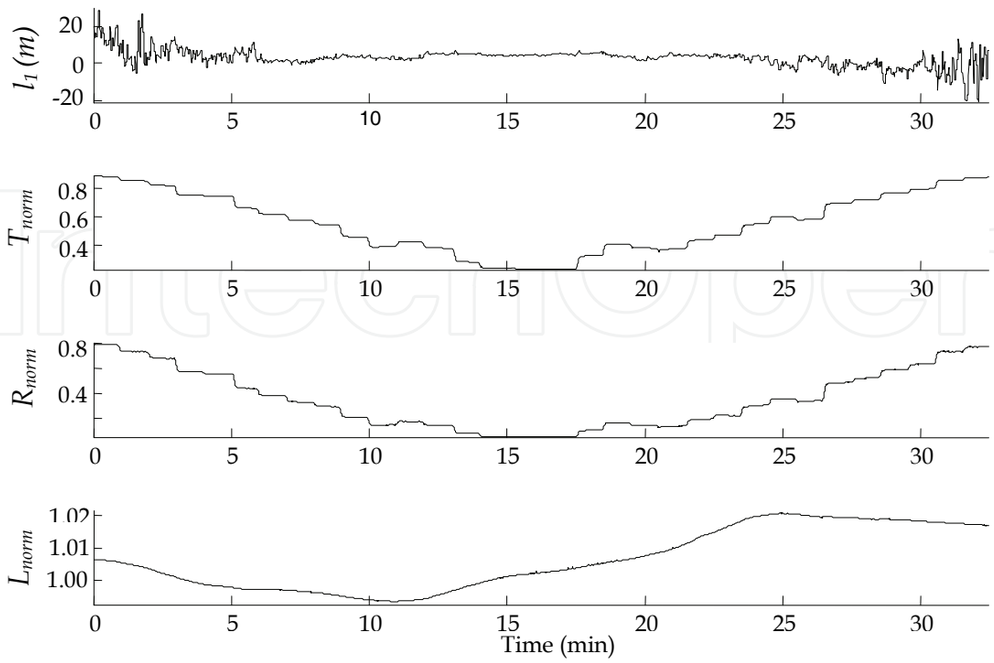

Fig. 15. Measurands variations for losses gradually induced near source-end of 1.3 km-length test fiber.

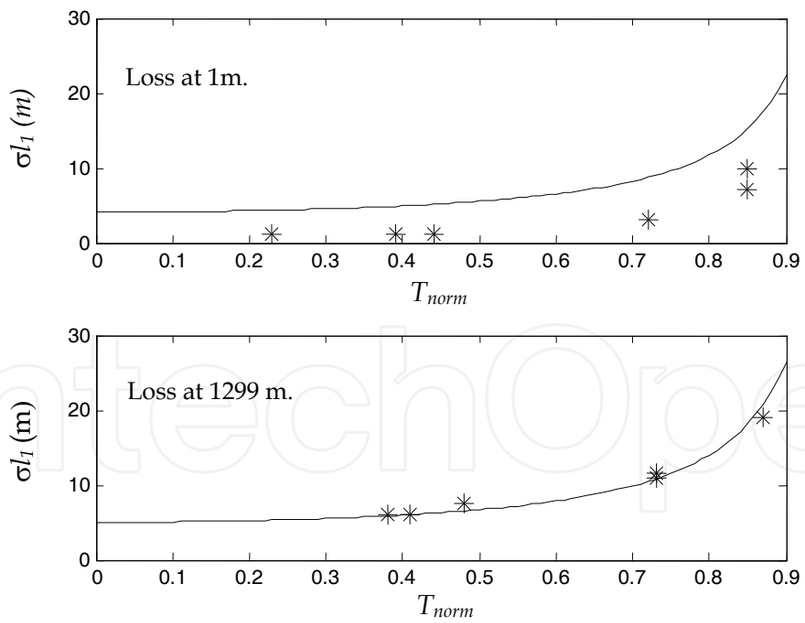

Fig. 16. Calculated (solid lines, σ_{Rnorm} = 0.0015 and σ_{Tnorm} = 0.0003) and measured (stars) localization error for 1.3 km-length test fiber.

Qualitatively the same results were obtained with 5.6 km-length SMF-28 test fiber. Fig.17 shows recorded with AMS-TRA measurands for the gradual change of the loss value. The losses were induced near the remote-end of 5.6 km-length test fiber. Note that in this case normalized Rayleigh backscattered power does not depend on value of losses.

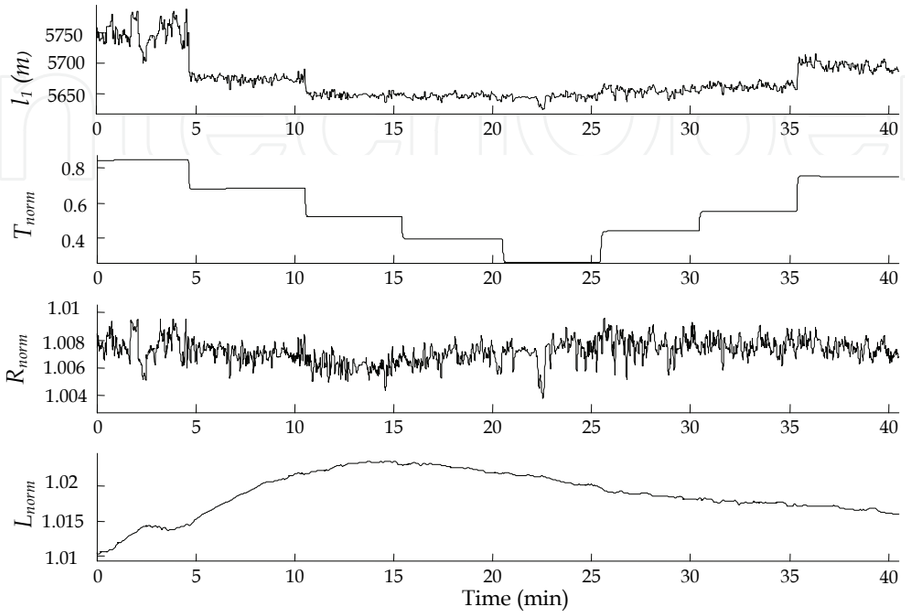

Fig. 17. Localization errors for losses induced near remote-end of 5.6 km-length test fiber.

Fig. 18 shows calculated and measured localization errors for 5.6 km-length test fiber.

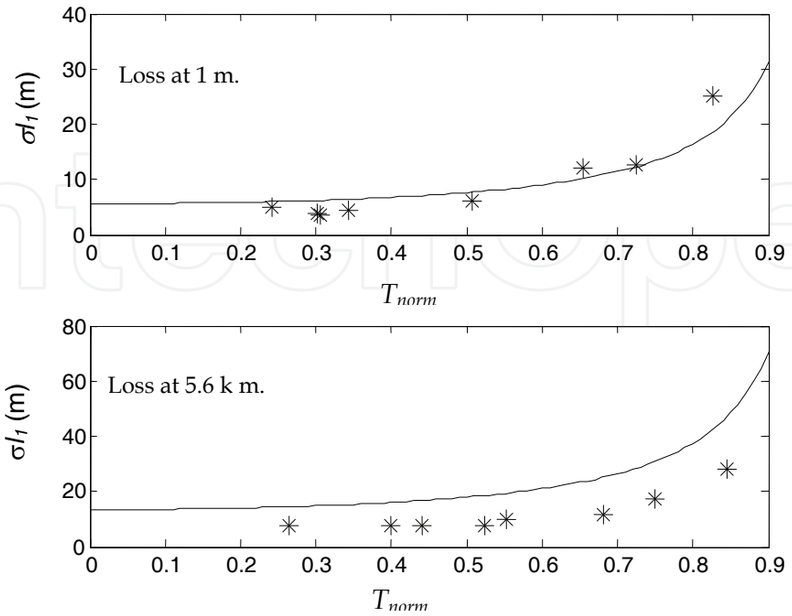

Fig. 18. Calculated (solid lines) and measured (stars) localization error for 5.6 km test fiber.

Variations of the disturbance location l_1 for the strong perturbations do not exceed ±10 meters for the losses induced near remote-end of the test fiber. Experimentally measured standard deviations of the normalized reflected and transmitted powers due to various instability in the prototype were $\sigma_{Rnorm} = 0.0025$ and $\sigma_{Tnorm} = 0.0003$ for signal bandwidth equal to 1 Hz. These data were used for the numerical estimation of the localization errors.

5.3 Gasoline Leak Detection and Localization

As well known gasoline does not affect optical fiber directly. In order to induce the losses under gasoline influence, special transducer with swellable polymer should be used. The design of the test cable with gasoline- sensitive transducer is shown schematically in Fig.19.

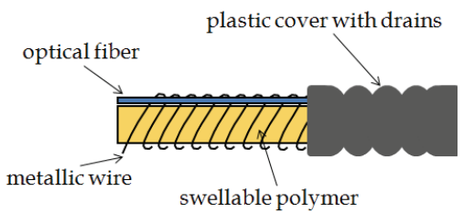

Fig. 19. Fiber optic gasoline-sensitive cable in detail.

The optical fiber and swellable polymer were coupled together mechanically by soft metallic wire winded around them. The fiber was placed inside small groove in the polymer that allows avoid undesirable inoperative losses, but does not significantly increase the response time of the sensor. A white butyl rubber was used as the swellable polymer in the sensitive cable. This material has good aging properties at elevated temperatures, good chemical stability. It also resists weathering, sunlight, ozone, mineral acids, oxygenated solvents (ketones and alcohols), and water absorption (Allen, 1972; Morton, 1987). Butyl rubber absorbs and swells in hydrocarbon media without dissolution and significant change of its mechanical property. The swelling behavior of the polymer produces an increase in the physical dimensions of the material, which can be readily converted to a mechanical response. Our study shows that butyl rubber can increase its volume by more than 2 times under gasoline influence (Spirin et al., 2000; Lopez et al., 2004). Furthermore, its behavior is reversible, i.e. the white butyl rubber can be used over multiple wet-dry cycles. In our experiment we tested the sensor under gasoline influence, but qualitatively the same swelling behavior butyl rubber shows in a range of hydrocarbon fuels (MacLean et al., 2001). The swellable polymer has tube shape with 25 mm diameter and metallic wire was winded with 5 mm spacing [López, 2002]. Fiber and polymer are protected by an outer plastic cover with drains for gasoline.

To study sensor response, part of sensitive cable located at 1300 meter from the source-end of the test fiber was placed inside a 20-cm length vessel filled with gasoline. Under gasoline influence butyl rubber swells and bends the fiber that induces the losses into the test fiber. Fig. 20. shows the change of transmission of the test fiber during wet-dry cycle. The decrease of transmission indicates gasoline presence and allows estimate an integral value of the disturbance.

Fig. 21. presents AMS-TRA prototype response on gasoline leak at 1300 meter distance. Under gasoline influence the transmission T_{norm} is decreasing and alarm signal is activated when transmission is became less than a threshold level equal to 0.9. With this particular sensitive cable the alarm level was achieved after 19 minutes of gasoline influence. Initial variation of alarm distance l_1 was ±32 meters for 0.5 dB losses and then decreasing to ±13 meters for 2 dB losses. For the losses more than 3 dB the variations not exceeds ±3 meters.

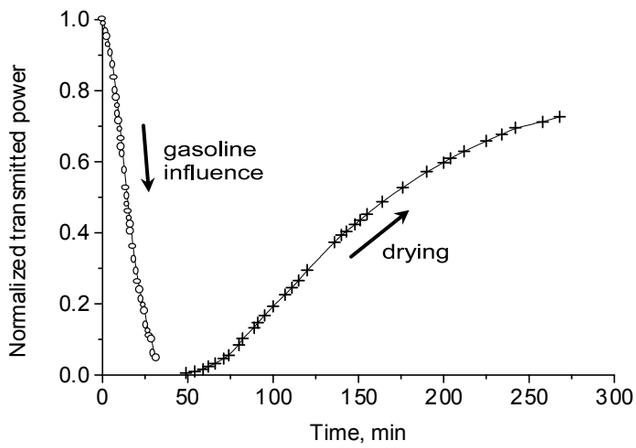

Fig. 20. Normalized transmitted power during wet-dry cycle (o - gasoline influence, + - drying).

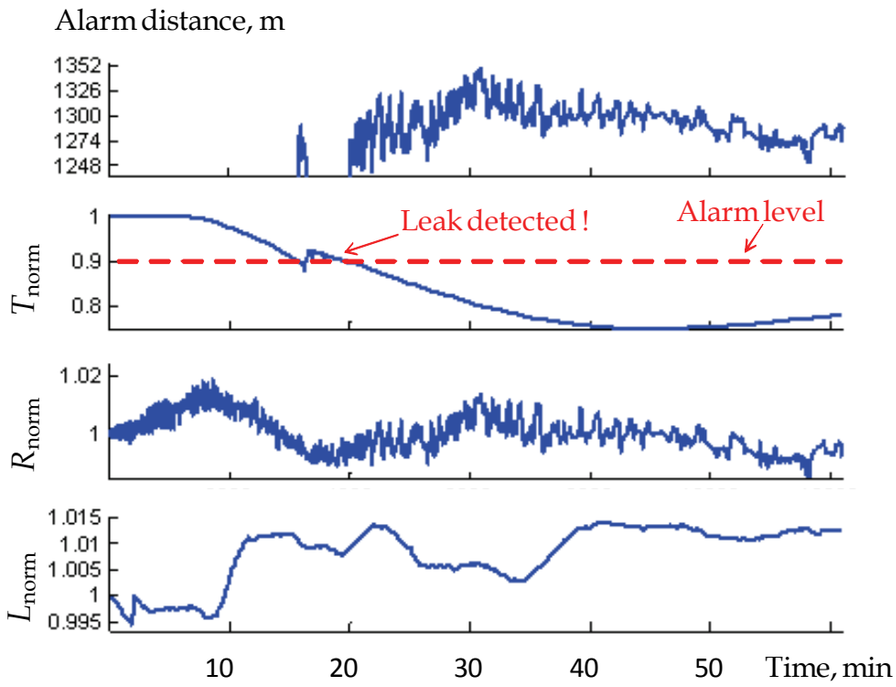

Fig. 21. AMS-TRA response on gasoline leak at 1300 meter.

6. Conclusion

We have demonstrated that the TRA method provides new opportunity for the localization of loss-induced alarm-like perturbation along few km-length test fibers by measuring transmitted and reflected powers of an unmodulated light.
We have designed completely autonomous measurement system based on transmission-reflection analysis. The autonomous system utilizes simple optical scheme with low-cost diode laser and original data acquisition and signal processing system. The AMS-TRA prototype demonstrates localization of loss-inducing perturbation along a 1÷6 km-length standard single mode SMF-28 fiber with few meters error for the losses that surpass 3 dB.
We have employed the AMS-TRA prototype with special sensitive cable for the gasoline leak localization. Alarm signal was activated after 15÷20 minutes of gasoline influence on 20 cm-length piece of sensitive cable which is located at the end of 1.3 km-length test fiber. For the losses more than 3 dB the variations of the alarm distance not exceeds ±3 meters.
We believe the proposed technique will be very attractive for the eventual realization of a compact and inexpensive distributed alarm fiber optic sensor.

7. Acknowledgement

We gratefully acknowledge financial support from the Consejo Nacional de Ciencia y Tecnología de México through Project 23770 SEMARNAT.

8. References

Hartog, A. (2000). Distributed fiber-optic Sensors: Principles and applications, In *Optical Fiber Sensor Technology*: *Advanced Applications-Bragg Gratings and Distributed Sensors,* edited by K.T.V. Grattan and B.T. Meggitt, pp. 241-302, Kluwer Academic Publishers, ISBN 0-7923-7946-2, Boston

Byoungho, Lee (2003). Review of the present status of optical fiber sensors. *Optical Fiber Technology,* Vol. 9, 2003, pp. 57–79**,** ISSN 1068-5200

Tsuji, K.; Shimizu, K.; Horiguchi, T. & Koyamada, Y. (1995). Coherent optical frequency domain reflectometry for long single-mode optical fiber using a coherent lightwave source and an external phase modulator, *IEEE Photonics Technol. Letters,* Vol. 7, 1995, pp. 804–806, ISSN 1041-1135

Pierce, S.G.; MacLean, A. & Culshaw, B. (2000). Optical frequency-domain reflectometry for microbend sensor demodulation. *Applied Optics,* Vol. 39, 2000, pp.4569-4581, ISSN 0003-6935

Venkatesh, S. & Dolfi, D.W. (1990). Incoherent frequency modulated cw optical reflectometry with centimeter resolution. *Applied Optics,* Vol. 29, 1990, pp. 1323-1326, ISSN 0003-6935

Spirin, V. V.; Shlyagin, M. G.; Miridonov S. V. & Swart, Pieter L. (2002a). Transmission/reflection analysis for distributed optical fibre loss sensor interrogation. *Electronics Letters*, Vol. 38, No. 3, 2002, pp. 117-118, ISSN 0013-5194

Spirin, V. V.; Shlyagin, M. G.; Miridonov, S. V. & Swart, Pieter L. (2002b). Alarm-condition detection and localization using Rayleigh scattering for a fiber optic bending sensor

with an unmodulated light source. *Optics communications,* Vol. 205, No. 1-3, 2002, pp. 37-41, ISSN 0030-4018

Gysel, P. & Staubli, R.H. (1990). Statistical Properties of Rayleigh Backscattering in Single-Mode Fibers", *J. Lightwave Technology* Vol**.** 8, 1990, pp. 561-567, ISSN: 0733-8724 Liaw, S.-K. ; Tzeng, S.-L. & Hung Y.-J. (2000). Rayleigh backscattering induced power penalty on bidirectional wavelength-reuse fiber systems, *Optics Communications,* Vol. 188**,** 2000, pp. 63- 67, ISSN 0030-4018

Brinkmeyer, E. (1980). Backscattering in single-mode fibers, *Electronics Letters, Vol.* 16**,** 1980, pp. 329- 330, ISSN 0013-5194

Beller, J. (1998). OTDRs and Backscatter Measurements, In: *Fiber Optic Test and Measurement*, edited by D. Derickson, pp. 434-474, Prentice Hall PTR, ISBN 0-13-534330-5, New Jersey

Spirin, Vasilii V. (2003) Transmission-Reflection Analysis for Localization of Temporally Successive Multipoint Perturbations in a Distributed Fiber-Optic Loss Sensor Based on Rayleigh Backscattering. *Applied Optics*, Vol. 42, No. 7, 2003, pp. 1175-1181, ISSN 0003-6935

Spirin, V. V.; Mendieta, F.J.; Miridonov, S. V.; Shlyagin, M. G.; Chtcherbakov, Anatoli A. & Swart, Pieter L. (2004) Localization of a loss-inducing perturbation with variable accuracy along a test fiber using transmission-reflection analysis, *IEEE Photonic Technology Letters.,* Vol. 16, 2004, pp. 569-571, ISSN 1041-1135

Spirin, Vasily V.; Miridonov, Serguei V.; Mitrani, Enrique; Morales, Carlos; Shlyagin, Mikhail G.; Castro, Marcial & Manriquez, Manuel. (2007). Autonomous measurement system for localization of loss-induced perturbation based on transmission-reflection analysis, In: Fiber Optic Sensors and Applications V, Proceedings of SPIE Volume: 6770, pp. 6770OH 1-9 ISBN 9780819469304

Allen, P. W. (1972). *Natural Rubber and the Synthetics*, 255 pages, John Wiley & Sons, ISBN: 0470023295, New York

Morton, M. (1999) *Rubber Technology*, 638 pages, Kluwer Academic Publishers, ISBN 0-412-53950-0, Netherlands

Spirin, V.V.; Shlyagin, M.G.; Miridonov, S. V. ; Mendieta, F. J. & López R. M. (2000) Fiber Bragg grating sensor for petroleum hydrocarbon leak detection, *Optics and Lasers in Engineering,* Vol. 32, 2000, pp. 497-503, ISSN 0143-8166

López, R.M. ; Spirin, V. V. ; Shlyagin, M.G. ; Miridonov, S.V. ; Beltrán, G. ;.Kuzin, E.A & Márquez Lucero, A. (2004). Coherent optical frequency domain reflectometry for interrogation of bend-based fiber optic hydrocarbon sensors. *Optical Fiber Technology*, Vol. 28, No. 10, 2004, pp. 79-90, ISSN 1068-5200

MacLean, A.; Moran, C.; Johnstone, W.; Culshaw, B.; Marsh, D. & G. Andrews. (2001). A distributed Fiber Optic Sensor for Liquid Hydrocarbon Detection, In: Smart Structures and Materials 2001: Sensory Phenomena and Measurement Instrumentation for Smart Structures and Materials, Proceedings of SPIE Vol. 4328,2001, ISBN 9780819440143

López, R. M.; Spirin, V.V.; Miridonov, S. V.; Shlyagin, M. G.; Beltrán, G. & Kuzin E.A. (2002). Fiber optic distributed sensor for hydrocarbon leak localization based on transmission/reflection measurement. *Optics&LaserTechnology,* Vol. 34, No. 6, 2002, pp. 465-469, ISSN 0030-3992

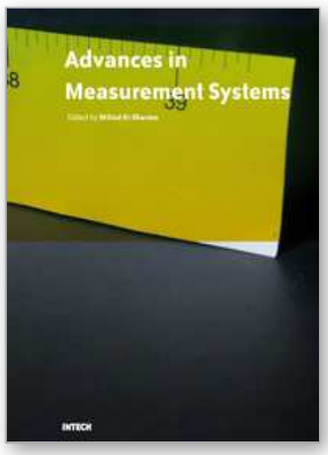

Advances in Measurement Systems

Edited by Milind Kr Sharma

ISBN 978-953-307-061-2
Hard cover, 592 pages
Publisher InTech
Published online 01, April, 2010
Published in print edition April, 2010

How to reference

In order to correctly reference this scholarly work, feel free to copy and paste the following:

Vasily V. Spirin (2010). Autonomous Measurement System for Localization of Loss-Induced Perturbation Based on Transmission-Reflection Analysis, Advances in Measurement Systems, Milind Kr Sharma (Ed.), ISBN: 978-953-307-061-2, InTech, Available from: http://www.intechopen.com/books/advances-in-measurement-systems/autonomous-measurement-system-for-localization-of-loss-induced-perturbation-based-on-transmission-re

INTECH
open science | open minds

InTech Europe
University Campus STeP Ri
Slavka Krautzeka 83/A
51000 Rijeka, Croatia
Phone: +385 (51) 770 447
Fax: +385 (51) 686 166
www.intechopen.com

InTech China
Unit 405, Office Block, Hotel Equatorial Shanghai
No.65, Yan An Road (West), Shanghai, 200040, China
中国上海市延安西路65号上海国际贵都大饭店办公楼405单元
Phone: +86-21-62489820
Fax: +86-21-62489821

IntechOpen